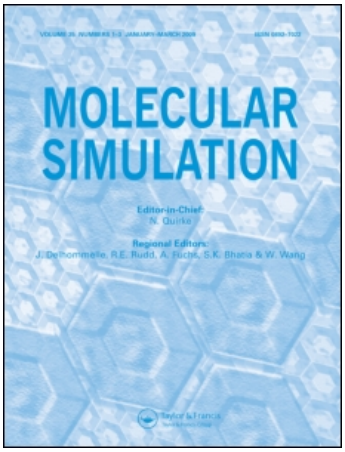

Molecular Simulation
Publication details, including instructions for authors and subscription information:
http://www.informaworld.com/smpp/title~content=t713644482

Molecular dynamics simulations of polyampholytes inside a slit

J. Feng[a]; H. Liu[a]; Y. Hu[a]
[a] Department of Chemistry and State Key Laboratory of Chemical Engineering, East China University of Science and Technology, Shanghai, China

To cite this Article Feng, J. , Liu, H. and Hu, Y.(2005) 'Molecular dynamics simulations of polyampholytes inside a slit', Molecular Simulation, 31: 10, 731 — 738
To link to this Article: DOI: 10.1080/08927020500237699
URL: http://dx.doi.org/10.1080/08927020500237699

Molecular Simulation, Vol. 31, No. 10, August 2005, 731–738

Taylor & Francis
Taylor & Francis Group

Molecular dynamics simulations of polyampholytes inside a slit

J. FENG, H. LIU* and Y. HU

Department of Chemistry and State Key Laboratory of Chemical Engineering, East China University of Science and Technology, Shanghai 200237, China

(Received November 2004; in final form February 2005)

Alternating and diblock polyampholytes confined in a slit with and without an electric field have been simulated by the molecular dynamics method with a Langevin thermostat. It is shown that the slit has a strong effect on the properties of the polyampholyte. The effect is stronger when the electric field is weak, or the temperature is not too high. When a polyampholyte chain moves close to the slit wall, its radius of gyration perpendicular to the wall becomes smaller but that parallel to the wall becomes larger. Owing to the confinement of the slit, the polyampholyte chain closer to the slit wall tends to lie on the wall and becomes more flat. The width of the slit has only a little influence on the properties of solutions near the slit wall, values of several physical statistics are very close with different widths. However, when the electric field strength is strong enough in a narrow slit, the obtained properties obviously differ.

Keywords: Polyampholytes; Molecular dynamics simulation; Multichain effects; Diblock polyampholyte

1. Introduction

Polyampholytes are charged polymers containing both positively and negatively charged monomers along the backbone. Due to the co-existence of two or more monomers with equal or opposite charge and the random distribution of charges, the properties of polyampholytes are different from that of the polyelectrolytes. The chain of polyampholyte may collapse into a globule owing to the attraction between the differently charged monomers, and its solubility in aqueous solution is small. If salts are added to the solution, the chains of polyampholyte become more expanded because of the screening effect. It is a great challenge to develop theories for polyampholyte solutions. Experiments and simulations can fill the present gap of understanding.

In recent years, many studies on polyampholyte solutions have been carried out. Higgs and Joanny [1] found that the globule volume formed by neutral polyampholyte chains increases when the concentration of salt ions becomes larger than that of the charges on the polymer. Non-neutral polyampholyte chains with a strong net charge behave as conventional polyelectrolytes. From theoretical study and computer simulation Kantor *et al.* [2–4] found that the chain configuration of random polyampholytes could be either compact or expanded dependent on the net charges of the polyampholyte chain. There exists a critical charge $Q_c \approx \sqrt{N}$. When the net charge of the polyampholyte chain exceeds this critical value, the chain extends to the expanded configuration otherwise it is compact. Everaers *et al.* [5] studied multichain effects in salt-free polyampholyte solutions at finite concentrations, and found that the single-chain theories are exponentially limited to small concentrations. Yamakov *et al.* [6] has studied the size R_g of random polyampholytes as a function of polyampholyte chain length N. Using the scaling theory a relation of $R_g \propto N^{1/2}$ was obtained. Different scaling relations include $R_g \propto N^{1/3}$ obtained by Higgs and Joanny and $R_g \propto N$ obtained by Kantor and Kardar. Extensive Monte Carlo simulations were also performed by Yamakov *et al.* [6] for the model systems. Schiessel and Blumen [7] studied the conformations of freely jointed polyampholytes in external fields and found that the end-to-end distance strongly depends on the distribution of charges along the chain. The conformation of alternating polyampholytes in strong external fields is highly sensitive to chain length N. For odd N, the polyampholyte collapses, whereas for even N the polyampholyte becomes extended. Latterly Soddemann *et al.* [8] studied the conformational properties of polyampholytes in external electric fields by molecular dynamics simulations and scaling theory, and found that polyampholytes with a small

*Corresponding author. Tel.: +86-21-64252921. Fax: +86-21-64252485. E-mail: hlliu@ecust.edu.cn

Molecular Simulation
ISSN 0892-7022 print/ISSN 1029-0435 online © 2005 Taylor & Francis Group Ltd
http://www.tandf.co.uk/journals
DOI: 10.1080/08927020500237699

total charge collapse into spherical globules. When the net charge exceeds a critical value, the chains are expanded. Winkler *et al.* [9] has also studied equilibrium properties of the polyampholyte solutions in electric fields and presented an analytically tractable model. They found that alternating polyampholyte chains exhibit expanded configurations in intermediate electric fields. Whether a collapse or a stretching occurs depends on the number of mass points in a strong electric field. For a continuous chain of polyampholytes with random charge density, the equilibrium properties in a strong electric field are dominated by the charge distribution along the chain.

Many theoretical works focused on the adsorption of polyampholytes on charged objects. Nets *et al.* [10] has studied theoretically the interaction of a random polyampholyte chain with charged planes, charged cylinders, and charged spheres. They found that a polyampholyte chain possessed with a spontaneous dipole moment could be adsorbed onto a charged object depending on the charge of the object, the chain length of the polyampholyte and the fraction of charged monomers. The addition of salt weakens the absorbance tendency but is proved to be necessary to adsorb similarly charged polyampholytes onto the charged object in the case of planes and cylinders. Long polyampholytes forms globules. Dobrynin *et al.* [11–14] studied the adsorption of polyampholyte chains at a charged planar surface and on a charged spherical particle by scaling theory and the self-consistent mean-field theory. The equilibrium polymer density profile was determined by the balance of the long-range polarization-induced attraction of polyampholytes to the charged objects and the monomer–monomer repulsion. The density profile could be divided into many different regimes in the adsorption diagram through characteristic distance parameters.

In addition to theoretical studies, there are also many computer simulations investigations. Tanaka *et al.* [15–17] studied the structures of a strongly coupled single chain and multichain random polyampholyte, as well as condensation, crystallization and swelling of random polyampholytes. For a single polyampholyte chain, three regimes of stretched, oblate, and spherical conformations were observed at high, medium, and low temperature, respectively. With multichain polyampholytes, the typical state at high temperature is a container-bound one-phase state of separated chains with a substantial void among them. The association and dissociation processes occur reversibly. A glass transition occurs when the temperature is lowered. The authors also studied the influence of the Coulomb coupling parameter Γ. Neutral polyampholyte collapses when $\Gamma > 1$, condenses to a cubic crystal when $\Gamma \gg 1$ with widely extensible bonds, but remains in an imperfectly ordered glass structure with finitely extensible bonds. Non neutral polyampholyte whose net charges exceeds $\sqrt{N}/2$ behaves as a polyelectrolyte, it consists of non-overlapped chains for $\Gamma > 1$, and shrinks to a noncharged polymer cluster for $\Gamma < 1$. Feng *et al.* [18] has studied the adsorption complexation of a polyampholyte chain and a charged particle via Monte Carlo simulation. When the charge density and size of the particle are small, the chain is adsorbed on the particle surface with an extended configuration. By increasing the charge density and the particle size, the polyampholyte chain is collapsed on the surface.

Most of the above studies were on unrestrained systems. There are many systems with restraints, especially in the tubes of organism. Bright *et al.* [19] studied the properties of polyampholyte chains attached on a parallel surface by molecular dynamic (MD) simulations. Khan *et al.* [20] studied the effects of adsorption of polyampholytes to charged surfaces in a restrained system. In this work, we apply the MD simulations to study the effects of slit width, temperature, and electric field strength on the system of alternating and diblock polyampholyte solutions inside a slit. The alternating and the diblock are the two extreme cases in the series of polyampholytes, where the charges in the former chain backbone are the most dispersed and in the latter most converged. The properties of the two polyampholytes are representative of almost all polyampholytes.

2. Molecular dynamics simulations

2.1 Details of simulations

We adopt the primitive model for polyampholyte solutions. In the MD simulation, we use the Langevin equation to consider both the viscous force from solvent and the stochastic force from the heat-bath as in Grest and Kremer [21]. This method has been successfully used in polyelectrolytes simulation [22]. The equation of motion is

$$\ddot{r}_i = -\nabla U_i - \gamma \dot{r}_i + W_i(t) \tag{1}$$

where γ is a friction coefficient set equal to 1 in all simulations. $W_i(t)$ is a random force acting on particle i at time t which satisfies the equation

$$\langle W_i(t) W_i(t') \rangle = \delta_{ij} \delta(t - t') 6 k_B T \gamma \tag{2}$$

U_i is the interaction energy of particle i with other particles

$$U_i = \sum\nolimits_{j \neq i} U_{ij} = \sum\nolimits_{j \neq i} (U_{ij}^{\mathrm{e}} + U_{ij}^{\mathrm{LJ}} + U_{ij}^{\mathrm{C}}) \tag{3}$$

where U_{ij}^{e} is the electrostatic interaction energy between particles i and j,

$$U_{ij}^{\mathrm{e}} = \frac{e^2}{4\pi\varepsilon_r\varepsilon_0} \frac{z_i z_j}{r_{ij}} \tag{4}$$

The size is finite in one dimension (such as Z), or considered as a quasi 2D system. The electrostatics can be evaluated by the quasi 2D Ewald summation [23]. However, the amount of calculation is much larger than that of 3D Ewald summation. Some approximation methods can be used for the quasi 2D electrostatic system [24,25]. Shelley and Pâtéy [25] extended the simulation box in the normal direction as an equation of empty space (see figure 1). Using the extension box the quasi 2D electrostatic energy and force can be evaluated by traditional 3D Ewald summation. Spohr [26] found that when the extension parts are five times of original box, the deviation between the approximate method and the accurate quasi 2D Ewald summation is very small.

U_{ij}^{LJ} in equation (3) is the cut and shift Lennard-Jones potential between particles i and j. We use a cut-off

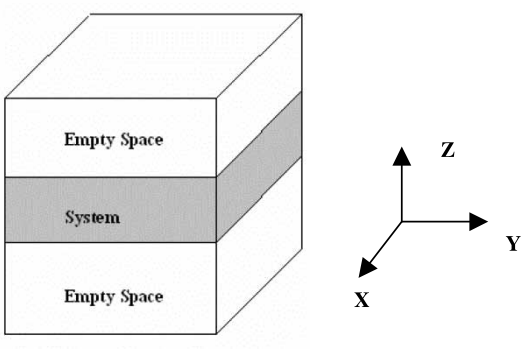

Figure 1. Extension simulation box for quasi 2D system.

distance $r_{ij}^c = 2^{1/6}\sigma_{ij}$, which is the excluded volume for all monomers.

$$U_{ij}^{\mathrm{LJ}} = \begin{cases} 4\varepsilon[(\sigma_{ij}/r_{ij})^{12} - (\sigma_{ij}/r_{ij})^6 - (\sigma_{ij}/r_{ij}^c)^{12} \\ \quad +(\sigma_{ij}/r_{ij}^c)^6] & r_{ij} \le r_{ij}^c \\ 0 & r_{ij} > r_{ij}^c \end{cases} \tag{5}$$

where, ε and σ_{ij} are energy and size parameters, respectively. The connectivity of nearest neighbor monomers in a chain is maintained by a finite extension nonlinear elastic (FENE) potential,

$$U_{ij}^{\mathrm{C}} = \begin{cases} -\frac{1}{2}kR_0^2 \ln(1 - r_{ij}^2/R_0^2) & r_{ij} \le R_0 \\ 0 & r_{ij} > R_0 \end{cases} \tag{6}$$

where, $k = 18\varepsilon/\sigma^2$ is the spring constant (in our simulations all the diameters of the particles is set equal to σ, i.e. $\sigma_{ij=}\sigma$), and $R_0 = 2\sigma_{ij}$ is the maximum extension. At these conditions the total fluctuation of chain length is about 5%.

The wall potential of the slit is the integrated Lennard-Jonnes potential [24].

$$U^w(z) = 2\pi\varepsilon\sigma^2\left[\frac{2}{5}\left(\frac{\sigma}{z}\right)^{10} - \left(\frac{\sigma}{z}\right)^4 + \frac{3}{5}\right], \; z \le \sigma_w \;\; = 0 \tag{7}$$

where, σ_w is the cut-off distance of a particle to a wall of the slit, and $\sigma_w = \sigma$. In most of the simulation systems the chain length of a polyampholyte chain is set equal to 32 and the chain numbers in the most simulations are 8. Initially, all these chains are inserted into the slit system randomly. The reduced number density ($\rho^* = \rho\sigma^3$) is 0.016. The product of reduced Bjerrum length ($e^2/4\pi\varepsilon_r\varepsilon_0 k_{\mathrm{B}}T\sigma$) and reduced temperature is 1. The time step is 0.015τ, and $\tau = \sigma\,(m/\varepsilon)^{1/2}$. The time steps of simulations are 3,000,000–4,000,000.

2.2 Structural properties [27]

For analyzing the effects of a slit, some structural properties parallel and perpendicular to the interface of the slit must be sampled. We mainly evaluate the following statistical averages of following properties.

Radius of gyration

$$R_g = \left\langle \left(\frac{1}{N}\sum_{i=1}^{N}[(x_i - x_c)^2 + (y_i - y_c)^2 + (z_i - z_c)^2] \right)^{1/2} \right\rangle \tag{8}$$

$$R_{g,p} = \left\langle \left(\frac{1}{N}\sum_{i=1}^{N}[(x_i - x_c)^2 + (y_i - y_c)^2] \right)^{1/2} \right\rangle \tag{9}$$

$$R_{g,v} = \left\langle \left(\frac{1}{N}\sum_{i=1}^{N}(z_i - z_c)^2 \right)^{1/2} \right\rangle \tag{10}$$

where, subscripts p and v mean parallel and perpendicular to the wall, respectively. Subscript c denotes the mass center of the chain molecule.

2.2.1 Gyration tensor. The gyration tensor is defined as

$$I_{\alpha\beta} = \sum_{i=1}^{N}\left(r_i^{\,2}\delta_{\alpha\beta} - r_{i\alpha}r_{i\beta}\right) \quad \alpha,\beta = x,y,z \tag{11}$$

Through the gyration tensor, three eigenvalues and eigenvectors can be obtained. The eigenvector corresponding to the maximal eigenvalue define the orientation of a molecule. Through the eigenvector can manipulate the molecule to include angle about the normal line of the slit interface.

2.2.2 Asphericity

$$\Delta = \sum_{i=1}^{3}\left(\lambda_i - \bar{\lambda}\right)^2/6\bar{\lambda}^2 \tag{12}$$

Through the three eigenvalues obtained by gyration tensor we also evaluate asphericity defined as which reflected the shape of the molecules.

3. Results and discussion

3.1 Slit without electric field

Figures 2–4 show the results of alternating and diblock polyampholytes inside a slit with a width of 20σ, in the absence of an electric field. The radius of gyration of alternating polyampholytes is larger than that of the diblock polyampholytes. This is because the electrostatic interaction inside the chain of diblock polyampholyte is larger than that of alternating polyampholyte. From figure 2 we can observe that when approaching the slit wall, the radius of gyration parallel to the wall increases slightly, while that perpendicular to the wall decreases notably. This resulted mainly from the repulsion of the wall. When a molecule is nearer the wall, it becomes more oblate and more parallel to the wall. As shown from figure 3, the asphericity and the angle about the normal line of the slit interface both increase when approaches to the wall. Figure 4 is the chain density profiles of the two polyampholytes, it shows that the distance from the wall within which the polyampholytes are affected is about

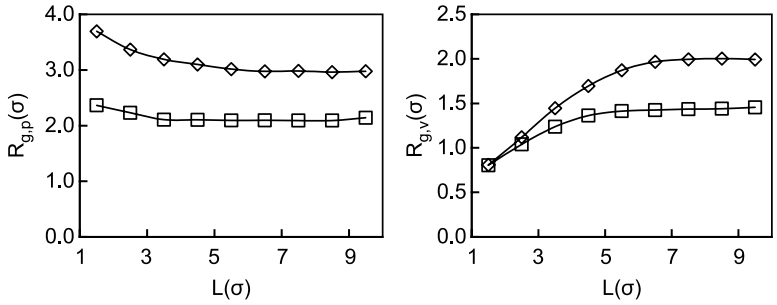

Figure 2. The profiles of radius of gyration measured parallel (left) and perpendicular (right) to the wall. Diamond: alternate; Square: diblock.

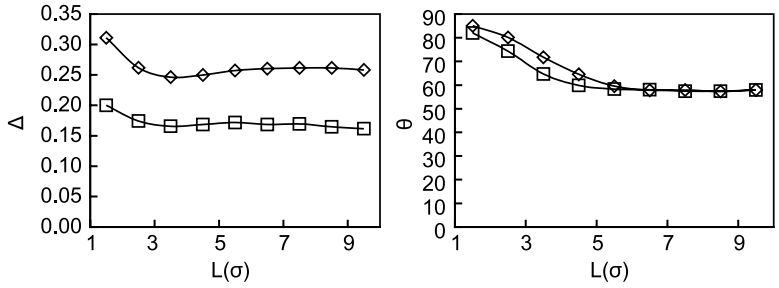

Figure 3. The profiles of the asphericity of chains (left) and the angle of chains vs. the wall (right). Diamond: alternate; Square: diblock.

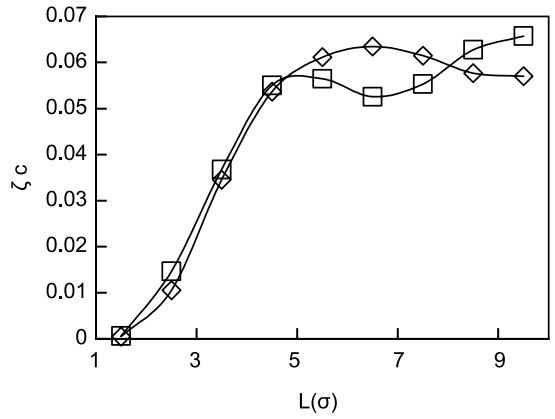

Figure 4. The chain-density profiles. Diamond: alternate; Square: diblock.

several segment diameters (in the example is about 5σ). The simulations verify that there is no changes in the profiles of the various quantities when $L = 8$, 12, 16, and 20 and all the variations are within 6σ from the wall.

Figures 5–7 show the effect of temperature. Generally, temperature increasing promotes the swelling of segments in chains. However from these figures we can see that the change is not obvious, which may be due to the overwhelming influence of the slit constraint.

3.2 Slit with the electric field

The configuration of polyampholytes is affected by the electric field. Figure 8 shows the effect of electric field strength on the radius of gyration of polyampholytes in single chain or multi-chain systems. The radius of gyration is linear with respect to the electric field strength

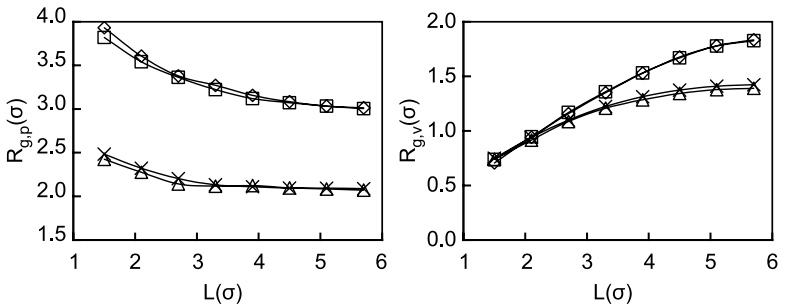

Figure 5. The profiles of radius of gyration of polyampholytes measured parallel (left) and perpendicular (right) to the wall. Diamond: alternate, $T = 1$; square: alternate, $T = 1.4$; Triangle: dibolock, $T = 1$; cross: diblock, $T = 1.4$.

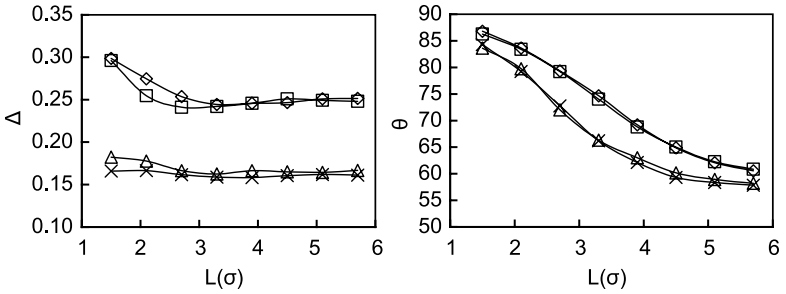

Figure 6. The profiles of the asphericity of polyampholytes (left) and the angle of polyampholytes vs. the wall (right). Diamond: alternate, $T = 1$; square: alternate, $T = 1.4$; Triangle: dibolock, $T = 1$; cross: diblock, $T = 1.4$.

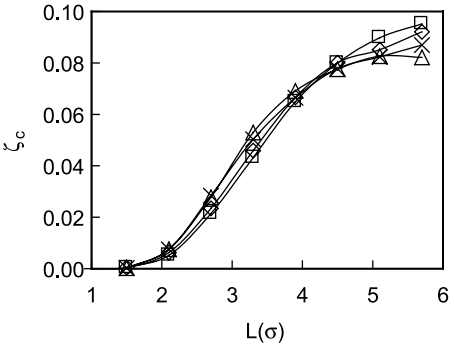

Figure 7. The chain-density profiles of polyampholytes. Diamond: alternate, $T = 1$; square: alternate, $T = 1.4$; Triangle: dibolock, $T = 1$; cross: diblock, $T = 1.4$.

as shown in the figure. In the single chain system, the effect follows $R_g \sim E^{0.6}$ for the alternating polyampholyte. For the diblock polyampholyte, there is a critical electric field at about 0.3, the radius of gyration shows discontinuity around this field. Before this critical field, the effect follows the same relation $R_g \sim E^{0.6}$ as that of alternating polyampholyte. In higher field after the critical, it is $R_g \sim E^{2.24}$. In the multi-chain system, owing to the interaction among the chains, the scale relations and the critical electric field strength are dependent on the density of polyampholytes, notably different from that of the single chain system. When the density is $\rho^* = 0.002$ and the scale relation is $R_g \sim E^{0.67}$ for alternating polyampholyte, $R_g \sim E^{0.54}$ for diblock polyampholyte in a low electric field and $R_g \sim E^{2.53}$ in a higher electric field.

Now we turn to the distance dependence of the properties against the wall on which the charges are carried. The slit width of systems is fixed at 12σ. Figures 9 and 10 are results of alternating polyampholytes. From these figures we find that the electric field strength affects the properties of alternating polyampholytes only slightly, even when the electric field strength is very strong. Alternating polyampholytes behave in a similar fashion to the polymer without charges. Figures 11 and 12 are for diblock polyampholytes. When the electric field strength is not strong, the influences are still not obvious. But when the electric field strength is very strong, diblock polyampholytes will be affected notably.

Figure 13 shows the results of diblock polyampholytes in the slit with different width at very strong electric field strength (the reduced electric field strength is 1). From the figure we find that, except for a very narrow slit such as 8σ, the properties at the given position have few relations with the width of a slit. It is different with those of alternating polyampholytes, and whose properties have few relations with the four kinds of width of a slit.

The behavior of polyampholyte in a slit is also affected by the solvent molecules and salt ions added to the solution. Figure 14 shows the effect of the salt density ρ_s on the radius of gyration of diblock polyampholyte, the density of polyampholyte is fixed at $\rho^* = 0.004$. The larger the salt density, the smaller is the radius of gyration due to the screening effect of the salt ions.

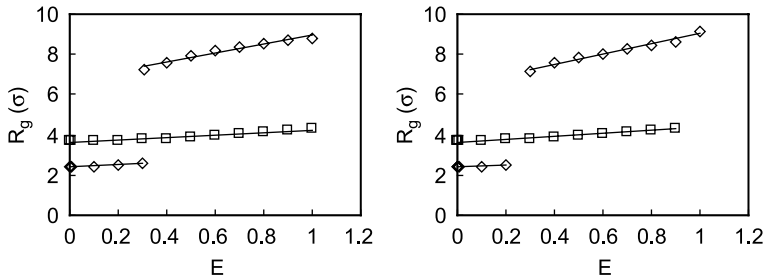

Figure 8. The effect of the electric field strength on the radius of gyration of polyampholytes. Single chain (left), Multi-chain (right). Diamond: diblock polyampholyte; Square: alternating polyampholyte.

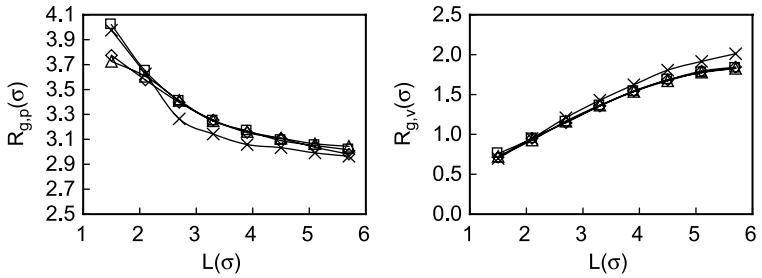

Figure 9. The profiles of radius of gyration of alternating polyampholytes measured parallel (left) and perpendicular (right) to the wall at various electric fields. Diamond: $E = 0.001$; square: $E = 0.01$; Triangle: $E = 0.1$; cross: $E = 1.0$.

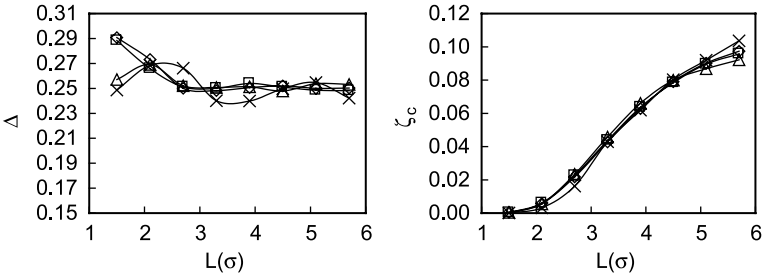

Figure 10. The profiles of the asphericity of alternating polyampholytes (left) and the chain-density profiles of alternating polyampholytes (right) at various electric fields at various electric fields. Diamond: $E = 0.001$; square: $E = 0.01$; Triangle: $E = 0.1$; cross: $E = 1.0$.

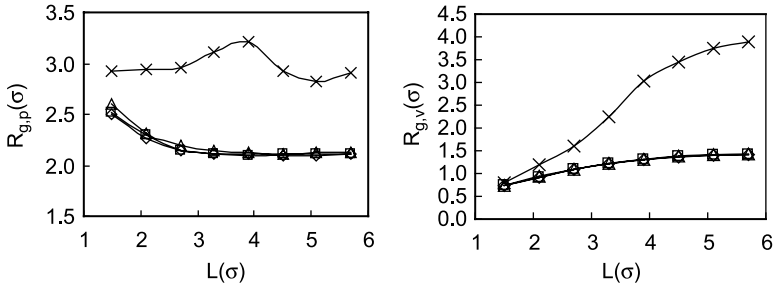

Figure 11. The profiles of radius of gyration of diblock polyampholytes measured parallel (left) and perpendicular (right) to the wall at various electric fields. Diamond: $E = 0.001$; square: $E = 0.01$; Triangle: $E = 0.1$; cross: $E = 1.0$.

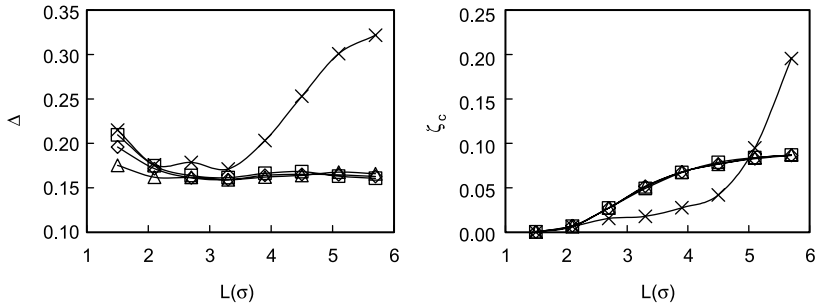

Figure 12. The profiles of the asphericity of diblock polyampholytes (left) and the chain-density profiles of diblock polyampholytes at various electric fields (right) at various electric fields. Diamond: $E = 0.001$; square: $E = 0.01$; Triangle: $E = 0.1$; cross: $E = 1.0$.

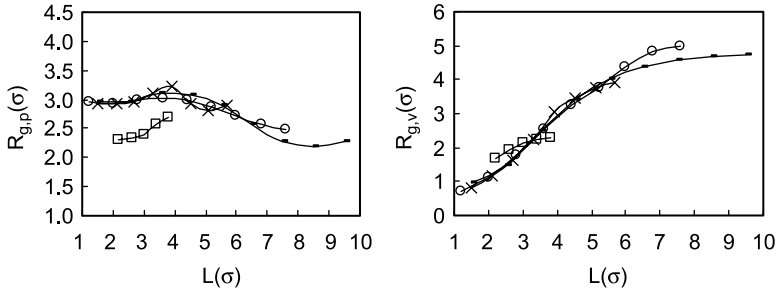

Figure 13. The profiles of radius of gyration of diblock polyampholytes measured parallel (left) and perpendicular (right) to the wall at various slit thickness. Diamond: $L = 8$; Triangle: $L = 12$; cross: $L = 16$; plus: $L = 20$.

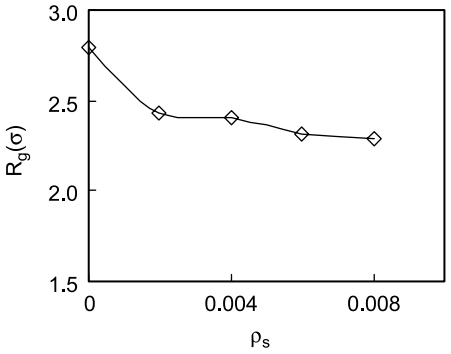

Figure 14. The effect of the salt density on the radius of gyration of diblock polyampholyte.

4. Conclusions

Although we have only studied the two specific cases, alternating and diblock polyampholytes, they are the extreme cases. We can obtain the behavior of the intermediate cases because, in most instances, the properties are similar for the two cases. From the MD simulations on alternating and diblock polyampholyte solutions inside slits, we have obtained some properties of polyampholytes in common. When the electric field of the slit system is weak or without the field and the temperature is not too high, the influence of the slit is predominant, the influence of the other factors can be ignored. When the molecule is close to the slit wall, the radius of gyration perpendicular to the wall becomes smaller but that parallel to the wall becomes larger. Owing to the restriction of the slit, the molecules closer to the slit wall are more parallel to the wall and become more flat. Within the width of several segment diameters, the closer to the slit wall, the less the density of the molecule is. In the region about 5σ away from the wall, the density of the molecule approaches a constant value. The properties of solutions near the slit wall have little relation with the width of the slit. However, when the electric field strength is strong enough in a narrow slit, the obtained properties differ greatly. It is notable that the model in our work belongs to the primitive model, where the solvent is treated as a continuous medium. When considering the solvent molecules explicitly the model is a non-primitive model. Due to the coulomb screening and solvation of the solvent in the non-primitive model, some properties related to electrostatic interaction may be different to those in the primitive model such as the scaling relations of the radius of gyration of polyampholytes with the external electric field strength. However, at fixed density and external electric field strength, or the slit width, the results by the primitive model may be similar to those of the non-primitive model at lower electric field strength.

Acknowledgements

This work is supported by the National Natural Science Foundation of China (Projects No.20236010, 20476025, 20490200), E-Institute of Shanghai High Institution Grid (No.200303) and the Shanghai Municipal Education Commission of China.

References

[1] P.G. Higgs, J.F. Joanny. Theory of polyampholyte solutions. *J. Chem. Phys.*, **94**, 1543 (1991).
[2] Y. Kantor, M. Kardar, H. Li. Statistical Mechanics of polyampholytes. *Phys. Rev. E.*, **49**, 1383 (1994).
[3] Y. Kantor, M. Kardar. Randomly charged polymers: An exact enumeration study. *Phys. Rev. E*, **52**, 835 (1995).
[4] Y. Kantor, M. Kardar. Instabilities of charged polyampholytes. *Phys. Rev. E*, **51**, 1299 (1995).
[5] R. Everaers, A. Johner, J.-F. Joanny. Polyampholytes: From single chains to solutions. *Macromolecules*, **30**, 8478 (1997).
[6] V. Yamakov, A. Milchev, H.J. Limbach, B. Dünweg, R. Everaers. Conformations of random polyampholytes. *Phys. Rev. Lett.*, **85**, 4305 (2000).
[7] H. Schiessel, A. Blumen. Conformations of jointed polyampholytes in external fields. *J. Chem. Phys.*, **104**, 6036 (1996).
[8] T. Soddemann, H. Schiessel, A. Blumen. Molecular-dynamics simulations of polyampholytes: Instabilities due to excess charges. *Phys. Rev. E*, **57**, 2081 (1998).
[9] R.G. Winkler, P. Reineker. Equilibrium properties of polyampholytes in electric fields. *J. Chem. Phys.*, **106**, 2841 (1997).
[10] R.R. Netz, J.-F. Joanny. Complexaton behavior of polyampholytes and charged objects. *Macromolecules*, **31**, 5123 (1998).
[11] A.V. Dobrynin, M. Rubinstein. Polyampholyte solutions between charged surface: Debye-Huckel theory. *J. Chem. Phys.*, **109**, 9172 (1998).
[12] A.V. Dobrynin, E.B. Zhulina, M. Rubinstein. Structure of adsorbed polyampholyte layers at charged objects. *Macromolecules*, **34**, 627 (2001).
[13] A.V. Dobrynin. Polyampholyte adsorption on a charged sphere. *Phys. Rev. E*, **63**, 0518021 (2001).
[14] E.B. Zhulina, A.V. Dobrynin, M. Rubinstein. Adsorption isotherms of polyampholytes at charged spherical particles. *J. Phys. Chem. B*, **105**, 8917 (2001).

[15] M. Tanaka, A. Yu Grosberg, V.S. Pande, T. Tanaka. Molecular dynamics study of the structure organization in a strongly coupled chain of charged particles. *Phys. Rev. E*, **56**, 5798 (1997).
[16] M. Tanaka, A. Yu Grosberg, T. Tanaka. Molcular dynamics of strongly coupled multichain coulomb polymers in pure and salt-added langevin fluids. *J. Chem. Phys.*, **110**, 8176 (1999).
[17] M. Tanaka, T. Tanaka. Clumps of randomly charged polymers: Molecular dynamics simulation of condensation, cystallization, and swelling. *Phys. Rev. E*, **62**, 3803 (2000).
[18] J. Feng, E. Ruckenstein. Monte Carlo simulation of polyampholyte-nanoparticle complexation. *Polymer*, **44**, 3141 (2003).
[19] J.N. Bright, M.J. Stevens, J. Hoh, T.B. Woolf. Characterizing the function of unstructured proteins: Simulations of charged polymers under confinement. *J. Chem. Phys.*, **115**, 4909 (2001).
[20] M.O. Khan, T. Åkesson, B. Jönsson. Adsorption of polyampholytes to charged surfaces. *Macromolecules*, **34**, 4216 (2001).
[21] G.S. Grest, K. Kremer. Molecular dynamics simulation for polymers in the presence of a heat bath. *Phys. Rev. A*, **33**, 3628 (1986).
[22] M.J. Stevens, K. Kremer. The nature of flexible linear polyelectrolytes in salt free solution: A molecular dynamics study. *J. Chem. Phys.*, **103**, 1669 (1995).
[23] D.M. Heyes, M. Barber, J.H.R. Clarke. Molecular Dynamics Coumputer Simulation of Surface Properties of Crystalline Potassium Chloride. *J. Chem. Soc Farad. Trans. H.*, **73**, 1485 (1977).
[24] J.B. Imbert, J.M. Victor, N. Tsunekawa, Y. Hiwatari. Conformation transitions of diblock polyampholyte in 2 and 3 dimensions. *Phys. Lett. A*, **258**, 92 (1999).
[25] J.C. Shelley, G.N. Patey. Boundary condition effects in simulation of water confined between planar wall. *Mol. Phys.*, **88**, 385 (1996).
[26] E. Spohr. Effect of Electrostatic boundary conditions and system size on the interfacial properties of water and aqueous solutions. *J. Chem. Phys.*, **107**, 6342 (1997).
[27] C. Mischler, J. Baschnagel, K. Binder. Polymer films in the normal-liquid and supercooled state: a review of recent Monte Carlo simulation results. *Adv. Colloid Interface Sci.*, **94**, 197 (2001).